THE JOURNAL OF PHYSICAL CHEMISTRY C
A JOURNAL OF THE AMERICAN CHEMICAL SOCIETY

pubs.acs.org/JPCC

Article

Modification of the Surface Structure and Electronic Properties of Diamond (100) with Tin as a Surface Termination: A Density Functional Theory Study

Sami Ullah* and Neil Fox

Cite This: J. Phys. Chem. C 2021, 125, 25165−25174

Read Online

ACCESS | Metrics & More | Article Recommendations

ABSTRACT: Many metal and metal oxide terminations have resulted in imparting negative electron affinity (NEA) to various diamond surfaces, especially diamond (100), and lowering the surface work function considerably. Tin, having many interesting properties in both metallic and oxide forms and being nontoxic and abundant, has the potential of being an efficient termination of diamond for interesting surface properties. Density functional theory is used to assess tin adsorption on the bare and oxygen-terminated diamond (100) surface. Quarter and half monolayer coverages of tin were found to be the most stable coverages in the case of both bare and oxygen-terminated diamond, resulting in large adsorption energies (up to −6.5 eV on the oxygen-terminated surface with an electron affinity up to −1.5 eV), comparable to the results obtained for H-terminated and alkali metal/metal oxide-terminated diamond surfaces. The electrostatic potential and density of states calculations suggest a stronger covalent bonding between the surface species along with the shift in the electron density toward or in the vicinity of surface carbon atoms, which leads to NEA. These results lay a foundation for any future investigation into this novel termination.

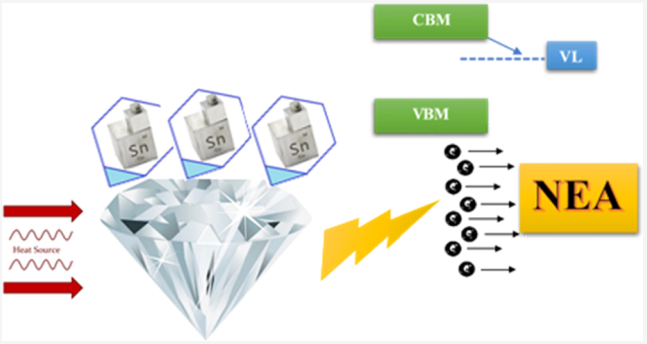

INTRODUCTION

Diamond, known for its strength and ornamental value, has drawn considerable interest in science and technology because of its superior electrical, thermal, mechanical, optical, and chemical properties, which can be used in novel applications such as thermionic emission, catalysis, quantum sensing, and so on.[1,2] An interesting contribution of diamond toward a much needed renewable energy generation technology would be the demonstration of low-temperature thermionic emission for thermionic energy conversion, which owes its existence to a property of certain diamond surfaces to exhibit negative electron affinity (NEA).[3] NEA exists when the vacuum level lies below the conduction level in a semiconductor material due to which there is a negligible energy barrier to electron emission. The existence of NEA on the surface of diamond has been attributed to the formation of a surface dipole between the surface carbon atoms and the terminating species.[4] The terminating species need to be a more electropositive atom or a group relative to the surface C atoms because of which the electron density shifts toward more electronegative C atoms and hence producing NEA. Achieving NEA in narrow-band gap semiconductors is difficult; however, in wide-bandgap semiconductors, like diamond, it is due to the natural proximity of the vacuum level to the conduction band maxima (CBM) that any suitable surface termination changes the surface dipole in such a way that the conduction band lies above the vacuum level. The existence of true NEA, where the CBM at the surface is higher than the local vacuum level, $E_{vac.}$ is crucial for achieving a significantly higher electron yield, which is desirable in applications like current amplifiers, vacuum electronics, thermionic converters, and even new forms of photochemistry.[5] True NEA can be differentiated from the effective NEA as in the latter case the CBM at the surface is very close to the vacuum level, which qualifies it for the positive electron affinity (PEA); however, because of sufficient downward band bending toward the surface deep in the bulk of the material, the CBM is above the vacuum level. This encourages the tunnelling of electrons from the CBM into the vacuum region without encountering a barrier if the space charge region is narrow enough.[6]

Received: July 5, 2021
Revised: October 18, 2021
Published: November 7, 2021

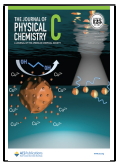

https://doi.org/10.1021/acs.jpcc.1c05973
J. Phys. Chem. C 2021, 125, 25165−25174

Also, the induction of NEA leads to the reduction in the ionization energy, a feature that is very critical to the surface transfer doping application used in many diamond-based electronic devices. Various atoms or groups have been explored as potential terminations of the diamond surface; some of them lead to the occurrence of PEA, while others impart NEA to various diamond surfaces with different orientations. Moreover, diamond has also been explored as an important material in quantum sensing application owing to the discovery of various elemental vacancy centers in it. Nitrogen-vacancy centers and silicon-vacancy centers with negative charge (as NV^- and SiV^-) have been explored in detail in different types of diamond materials, such as nanodiamonds, as candidates of interest in such applications. NEA would neutralize the negatively charged NV^- and SiV^- species, hence giving rise to the need for having a positive electron affinity diamond surface (PEA) that can preserve the charge state of vacancies in the diamond.[2]

Various atoms or groups have been investigated as potential PEA and NEA-terminating species to the diamond surfaces with various orientations. The most common PEA and NEA-imparting atoms that have been researched widely are oxygen (O) and hydrogen (H), respectively.[7−13] O-terminated diamond (OTD) surfaces have been researched widely as a PEA-imparting surface termination.[4] Many processes with diamond as simple as acid-washing result in the O surface termination of diamond.[14] Experimentally, O has been seen to occupy a mix of both the ether and the ketone (carbonyl) positions. Theoretically, ether-terminated diamond has been found to be the most stable form of OTD as has been found in our study as well. OTD has been seen to possess a PEA of up to 2.7 and 3.8 eV with large adsorption energies per atom in the case of ether and ketone terminations, respectively.[13,15−17] Experimentally, we have found the PEA value of 0.89 eV per atom for OTD.[18] This has resulted in O being studied as a potential candidate in quantum sensing and electrochemical applications along with other elements like boron[19,20] and so on. H termination of diamond has been found to possess an NEA of −1.96 eV theoretically and −1.3 eV experimentally.[19,21−27] However, hydrogen has been seen to desorb at elevated temperatures (≥700 °C) which renders it nonusable in the devices operating at high temperatures. Various metal and metal oxide terminations of diamond surfaces have been explored,[28,29] backed by the fact that oxygen inclusion results in the formation of stronger surface dipoles because of the increased sticking coefficient between the metal atom and the surface carbon atom.[5,30] Research has mostly focused on a certain group of elements as potential termination of the diamond surface. Alkaline metals, alkaline-earth metals, and transition metals have been a focus of most studies both theoretically and experimentally.[3,6,10,31−35] There are only a few studies that have focused on other elements like Al, Si, Ge, F, Sn, and so on,[18,30,36−39] which have been shown to impart NEA to the diamond surface. The same-group elements with Sn like Si and Ge have experimentally been studied as the surface terminations on diamond (100). Ge has been found to impart an NEA of −0.71 eV on the surface of diamond (100)[39] while Si deposition on the surface of diamond (100) has resulted in an electron affinity of −0.86 ± 0.1 eV; however, both Si and Ge have been determined to be unsuitable for device application under ambient conditions because of the high reactivity of unsatisfactory silicon and germanium bonds which would demand a protective layer to be grown on top of the structure (e.g., in the form of a SiO_2 layer), which could have a negative impact on NEA and a lower work function (WF) in these structures. Sn has also been experimentally observed to impart NEA on the surface of diamond (100) while being stable under ambient conditions which is a crucial point as far as device application of these structures is concerned. Table 1 shows the results of most stable terminations along with their corresponding EAs.

Table 1. Most Stable Coverages of Different Metals on the Various Orientations of Diamond and Their Corresponding Adsorption Energies along with Electron Affinities Taken from refs 19, 40, 41[a]

coverage (ML)	adsorbate	substrate	E_{ads} (eV)	χ (eV)
0.5	Al	bare	−3.97	−0.93
1	Al	bare	−4.11	−1.47
1	B	bare	−6.85	−1.39
1	Ti	bare	−5.08	0.35
1	Cu	bare	−2.93	−0.55
0.5	Al	OTD	−6.36	−0.37
1	Al	OTD	−4.58	−0.54
0.5	B	OTD	−9.0	0.49
1	Li	OTD	−3.64	−3.50
1	Na	OTD	−1.62	−1.42
0.5	Mg	OTD	−3.92	−2.77
0.5	Na	OTD	−2.41	−1.30
0.5	K	OTD	−1.92	−1.31
0.25	Cs	OTD	−2.19	−2.41

[a]Here, bare means unterminated diamond, while OTD represents oxygen-terminated diamond.

We are focusing on tin (Sn), a metal that has been left out as a potential termination of the diamond surface. Sn is available in abundance, nontoxic and has the same valency as carbon (C), hence lesser chance for lattice mismatch between Sn and C layers. Sn with a large electron cloud is expected to contribute to the redistribution of electron density toward more electronegative C and O because of which a surface dipole is generated with the negative side of the dipole inclined toward the surface carbon atoms, a strong reason for the generation of NEA on the surface of diamond. Sn adsorption on an OTD would also result in the formation of tin monoxide (SnO) on the surface of diamond. SnO has already been studied as a superior 2D material possessing various remarkable features, and its conductivity can be altered using different doping approaches. Moreover, lithiated tin has been shown to possess a remarkably lower WF in bulk form (as alloys). Hence, SnO-terminated diamond would not only lead to modification of diamond surface properties impressively but also encourage other studies of combining alkali metals like Li with SnO thin films for revolutionary properties on the surface of diamond for various applications. All of this emphasizes the significance of this work.

METHODS

A symmetrical 12-carbon-atom-thick periodic (in x and y) slab of carbon atoms, representing diamond (100), with 2 × 2 supercells on both (100) surfaces yielding four C atoms on each surface was used.[42] This enabled us to vary the coverage of Sn atoms from quarter monolayer (QML = 0.25 ML) to half monolayer (HML = 0.5 ML), to full monolayer (FML = 1 ML) by adsorbing one, two, or four Sn atoms, respectively. For

https://doi.org/10.1021/acs.jpcc.1c05973
J. Phys. Chem. C 2021, 125, 25165−25174

OTD, eight oxygen atoms were used to terminate the eight carbon atoms on both surfaces in ether and ketone configurations. The slab dimensions were fixed at 5.016 5 Å × 5.016 Å with a sufficient vacuum gap of 20−25 Å (~24.27 Å) in between the repeating cells such that the electrostatic potential (EP) had fully decayed in the vacuum. These slabs were used as the samples for experiments on the Cambridge Serial Total Energy Package (CASTEP) code[43] for performing the plane-wave density functional theory (DFT) calculations using Perdew−Burke−Ernzerhof generalized gradient approximation (GGA) for the exchange-correlation functional[44] and Vanderbilt pseudopotentials.[45] The plane-wave basis set of cut-off energy 700 eV along with a Monkhorst−Pack[46] mesh with 6 × 6 × 1 k-points (18 k-points in total) was used for geometric optimization while a 12 × 12 × 1 k point grid was employed for density of states calculation using the OptaDOS code[47] (using adaptive broadening of DOS peaks and a spacing of 0.07 eV as optimized in refs 30, 36.). The BFGS algorithm resulted in a geometry-optimized structure with tolerances of 0.05 eV/Å and 2×10^{-5} eV per atom in ionic forces and total energy, respectively.

In this work, all the adsorption energies were calculated with respect to the clean unterminated diamond surface to enable a comparison between the various terminations using the equation.[48,6]

$$\Upsilon = (E_T - E_o - (N_A \times E_{iso,A} + N_B \times E_{iso,B}))/N_T$$

where E_T and E_o represent the total energy of the terminated surface and clean diamond surface, while N_A and N_B are the number of adsorbate atoms of elements A and B, respectively. $E_{iso,\ A}$ and $E_{iso,\ B}$ are the energies of isolated adsorbate atoms of element A and element B, respectively, and N_T is the total number of adsorbate atoms. E_T, E_o, and $E_{iso,}$ are all negative; hence, the exothermic adsorption energies are negative as a convention in this work. The electron affinity (χ) is calculated using the equation:[6,3]

$$\chi = I - E_g$$

$I = (V_{vac} - V_{av,\ slab}) - (V_{VBM,\ bulk} - V_{av,\ bulk})$where I is ionization energy calculated by the method of Fall et al.[48] in this work and E_g is the experimental band gap value used (E_g = 5.47 eV) because of well-known underestimation of the band gap of diamond by the GGA method.[30] The energy difference between the vacuum potential and the average potential in the middle of the slab (bulk like) is represented by (V_{vac} − $V_{av,\ slab}$), which is obtained by performing the EP calculation on the slab. ($V_{VBM,\ bulk}$ − $V_{av,\ bulk}$) is the energy separation between the average EP energy in the bulk and the bulk valence band maximum, which can be obtained by performing a band structure calculation of bulk diamond. In semiconductors, the dopants and surface states alter the position of the Fermi level away from the center of the band gap and hence make it complex to compute the *WF* unlike the ionization energy (I), which depends upon the surface states only.

The experiments with the Sn-terminated diamond preceded by the validation calculations performed on the O- and H-terminated diamond which were then compared to the already available literature. Table 2 shows that the results from previous experiments agree with the results from this experiment.

Table 2. Electron Affinity (χ) and Adsorption Energy (E_a) for Various Diamond Surfaces[a]

sample	source	E_{ads} (eV)	χ (eV)
clean C	this work		0.73
	previous DFT		0.51−0.69,[15] 0.62,[17] 0.8,[6] and 0.28[51]
H T D	this work	−4.16	−1.9
	previous DFT	−4.14,[30] −4.54[52]	−1.95,[17] −2,[15] and −2.2[53]
OTD ether	this work	−7.16	2.74
	previous DFT	−8.2[17] and −6.21[12]	2.61−2.7[54] and 2.63[17]
OTD ketone	this work	−6.78	3.73
	previous DFT	−7.88[17] and −5.77[19]	3.75[17] and 3.64[54]

[a]Compared to the earlier studies as presented in the studies,[49,50] the values were found to be comparable.

RESULTS AND DISCUSSION

Before performing calculations on the actual metal, that is, Sn on diamond (100), the slabs were tested for convergence at different cut-off energies and k-points. The structural calculations were converged using a cut-off energy value of 700 eV, a Monkhorst−Pack grid of (6 × 6 × 1) k-points with a geometry convergence criterion (tolerances) of 0.05 eV/Å and 2×10^{-5} eV per atom in ionic forces and total energy, respectively, a fixed unit cell and no restrictions on atomic positions. The energy was seen to converge fairly with the parameters used. The energy minimization through geometry optimization and EP calculations were performed on bare, H-terminated, and OTD (both ether and ketone) surfaces (Table 2), which agree with the already available reports on these surfaces in the literature, hence demonstrating the viability of these parameters used for the future calculations.

After optimizing and confirming the parameters, it was deemed necessary to select the sites of adsorption for Sn atoms on diamond (100) surface. Most of the studies have adopted the traditional Levine structure to determine the high-symmetry adsorption sites on the surface of Si and diamond.[55] A few studies have chosen other sites as well.[42,19] This gave rise to a curiosity to test many other possible sites along with the abovementioned sites at various coverages of Sn on diamond (100). Figure 1 shows the general structure of 2 × 1 reconstructed and unreconstructed diamond surfaces along with the different sites for Sn adsorption.

Sn on Bare Diamond. As has been mentioned earlier, four Sn atoms on top of the surface with four C atoms give one FML adsorption. Hence, 0.25 ML would need one Sn atom anywhere on the four sites shown in Figure 1. However, for HML adsorption of Sn on diamond, two Sn atoms take up different combination of sites which are mentioned in Table 3. For one ML, there are only two most favorable ways (ether and ketone) in which Sn atoms could be placed on top of the diamond surface. Ether and ketone configurations in the case of FML coverage refer to the position of Sn atoms in between the surface C atoms and on top of surface C atoms, respectively. The unreconstructed surface of diamond (100) was found to be favorable for FML termination as it favors the bonding between Sn and C atoms due to the similar valency of the surface species. Any attempt to adsorb a FML of Sn in a different configuration or on a reconstructed diamond structure would output a HML-terminated diamond with

https://doi.org/10.1021/acs.jpcc.1c05973
J. Phys. Chem. C 2021, 125, 25165−25174

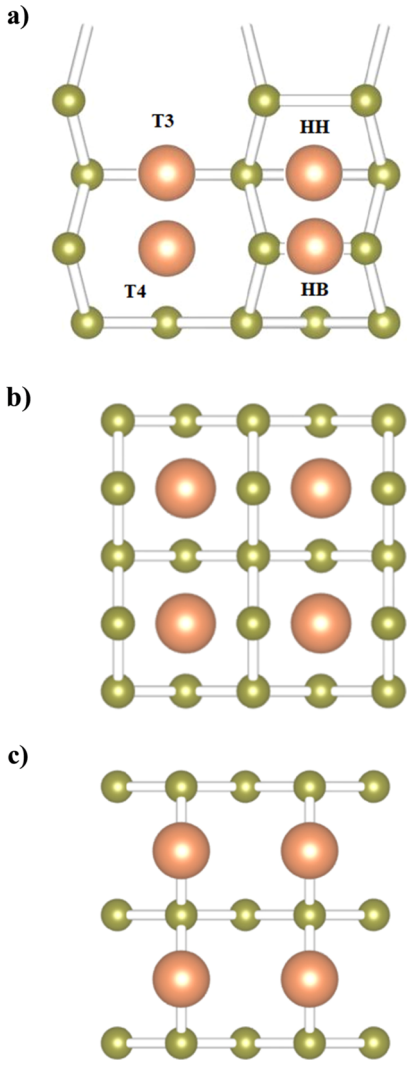

Figure 1. (a) Plan view of the bare (2 × 1) reconstructed diamond surface showing the potential high-symmetry adsorption sites for Sn on the bare diamond surface. HH, HB, T3, and T4 refer to the hexagon hole, hexagon bridge, third-tier carbon, and fourth-tier carbon sites, respectively. Green balls represent carbon atoms while orange balls represent tin atoms. (b) Unreconstructed diamond (100) surface with Sn atoms in the ether configuration (bridge position). (c) Unreconstructed diamond (100) surface with Sn atoms in the ketone configuration (on top position).

two Sn atoms unbonded which, in our opinion, satisfies the valency of both C and Sn atoms on the surface of diamond.

[a] Unreconstructed diamond structure.

Hence, it can be concluded through the information presented in Table 3 that the most favorable adsorption site in the case of 0.25 ML of Sn on diamond (100) is the T4 site (Figure 2a) where the highest adsorption energy of −4.27 eV with an NEA of −0.39 eV is obtained. For the HML case, the most stable and favorable site for Sn atoms is T4T4 (Figure 2b) with an adsorption energy value of −4.4 eV and a NEA value of −1.43 eV. As can be seen from Table 3, many other adsorption sites relaxed to T4T4 which indicates, again, this configuration to be the most stable and favorable one. Because of the large size of Sn atoms and the heavy electron cloud, there is a possibility of interatomic repulsion between Sn atoms which makes it relatively unfavorable for Sn atoms to achieve a full monolayer coverage on the diamond surface, hence giving

Table 3. Values of Electron Affinity, χ, and Adsorption Energy, E_{ads}, Calculated for Various Positions and at Different Surface Coverages of Sn on the Bare Diamond (100) Surface

coverage (ML)	input sites	output	adsorption energy, E_a (eV)/adsorbate	electron affinity, χ (eV)
0.25	HH	HH	−3.45	−0.58
0.25	HB	HB	−3.8	−0.8
0.25	T3	T3	−3.8	−0.89
0.25	T4	T4	−4.27	−0.39
0.5	HHHH		−4.2	−0.75
0.5	HBHB		−3.75	−1.6
0.5	T3T3		−3.2	−1.0
0.5	T4T4		−4.4	−1.43
0.5	HHHB		−4.29	−1.12
0.5	T3HB	T4HB	−4.3	−0.73
0.5	T3HH		−4.1	−1.01
0.5	T4HB		−4.3	−0.66
0.5	T4HH	T4HB	−4.3	−0.73
0.5	T4T3	T4T4	−4.4	−1.43
1	ETHER[a]		−1.9	−1.07
1	KETONE[a]		−2.14	−1.14

a very small value of adsorption energy for both ketone and ether positions. All other attempts to terminate the diamond surface with a full monolayer coverage in different configurations resulted in the output structure relaxing into the HML-terminated one with two Sn atoms left unbonded.

Figure 3 shows the EP for the HML (0.5 ML) of Sn on bare diamond (100), which shows the variation of EP along the normal axis to the surface. The negative and positive sides of the dipole can be visualized in the form of crests and trough (or upswings and downswings by convention), respectively. The negative side of the dipole is present toward (or on) the surface carbon atoms while the positive side of the dipole exists on Sn atoms. This dipole formation has been described as the source of NEA on the surface of diamond.[4]

Mulliken bond population analysis is widely used to assess the bond nature between any two species. A value of 0 indicates a perfectly ionic bond while an increasing value of bond population indicates increasing levels of covalency. In our case, the most stable HML adsorption exhibits the covalent nature of the bond between the surface C atoms and the adsorbed Sn atoms with a bond population value of 0.45. The adsorption of Sn atoms leads to an increase in the C−C dimer bond length from nearly 1.38 to 1.7 Å, which is expected because of the charge transfer between the C and Sn atoms and shows the dipole formation between more electropositive Sn atoms and the surface C atoms (C^-−Sn^+), also revealed by the Mulliken charge analysis, which shows that Sn gains a positive charge of 0.37*e* and 0.57*e*, while the C atoms gain a charge of −0.20*e* again confirming the charge transfer between the surface species. In the case of HML and FML adsorption, a similar trend can be seen which indicates preferential covalent nature of Sn to surface C bonds.

Sn on OTD. To achieve a full coverage of oxygen on the surface of diamond, eight oxygen atoms terminated both surfaces of diamond slab in ether and ketone configurations. Although it has been established widely using experimental and theoretical models that the ether configuration is the most stable one,[49] there are a few reports which mention the ketone configuration as the most favorable termination of diamond.[50]

https://doi.org/10.1021/acs.jpcc.1c05973
J. Phys. Chem. C 2021, 125, 25165−25174

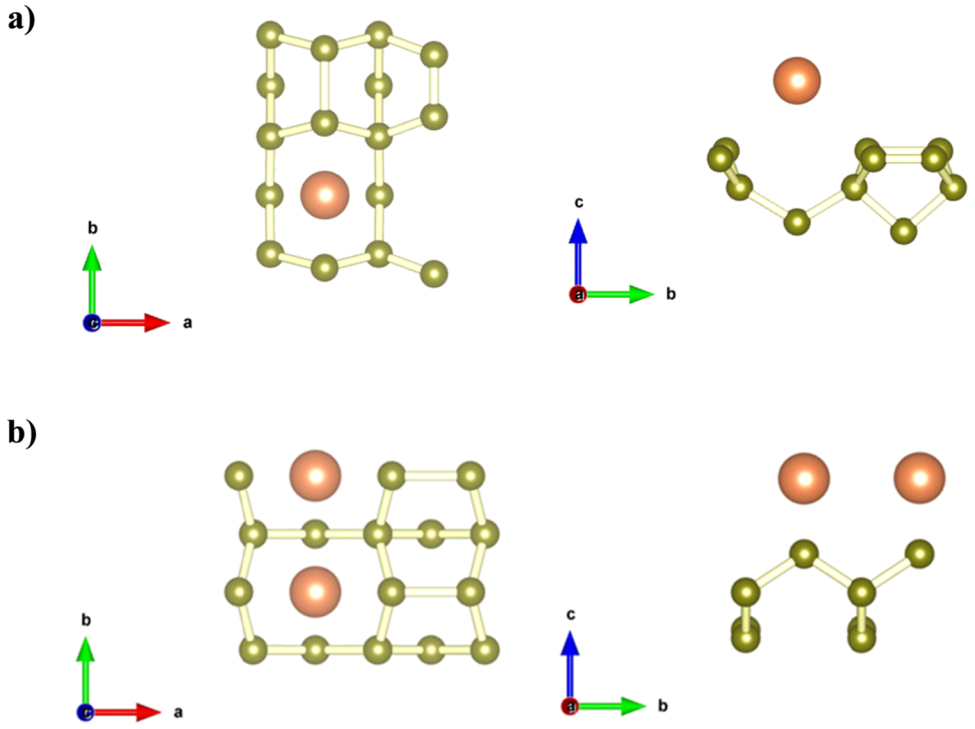

Figure 2. Most stable (a) QML and (b) HML of Sn on diamond (100). Note that the reconstruction of the diamond surface has occurred because of Sn adsorption. Green balls represent carbon atoms while orange balls represent tin atoms.

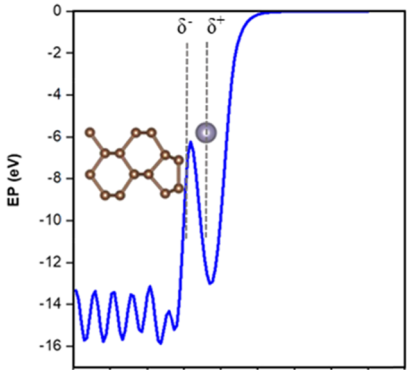

Figure 3. EP for the most stable configuration, i.e., HML of Sn on bare diamond (100). The EP is atom-centric like H termination instead of bond-centric as seen in the case of metal oxide (LiO) terminations of diamond. Here, brown balls represent carbon atoms and gray balls represent tin atoms.

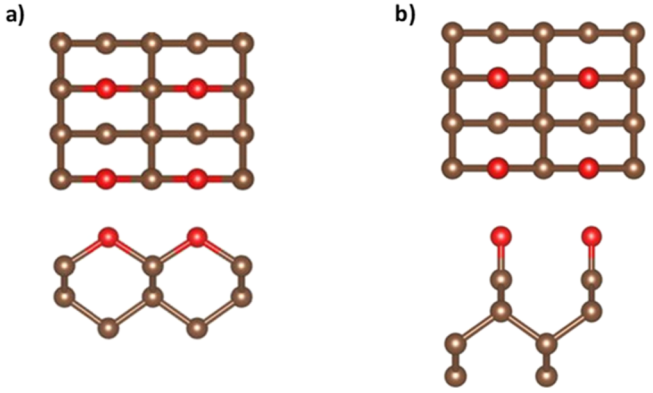

Figure 4. Clean diamond surfaces terminated with oxygen in (a) ether (bridge between two C atoms) and (b) ketone (on top of each C atom) configurations. Brown balls represent carbon atoms while red balls represent oxygen atoms.

In our study, the ether configuration of oxygen termination came out to be the most stable one. However, when it comes to metal oxide termination of diamond, it has been found that metals can easily break the ketone bonds between surface carbon and oxygen atoms to form metal oxide on the surface of diamond with surface C atoms dimerizing to reconstruct the diamond surface.[30] Thus, to establish which configuration of oxygen termination favors Sn deposition on the surface of diamond, both ether- and ketone-terminated surfaces were constructed and tested. Sn coverage varies in a similar manner as in the case of the bare diamond surface, that is, 0.25 ML or QML is represented by one Sn atom on each surface, while 0.5 ML or HML by two Sn atoms and one ML or FML by four Sn atoms on each surface of diamond (100). Figure 4 shows the ether and ketone clean unterminated diamond surfaces. The Sn atoms were placed on top of both the surfaces in different configurations and coverages which can be shown in Tables 4 and 5. Here ether and ketone with regard to Sn mean the bridge site (between two O atoms) and on top (of O atoms) site, respectively.

The ether bond being stronger and hence resilient to break with Sn adsorption yields lesser values of adsorption energy. A QML of Sn on the ether-terminated diamond (Figure 5a) is favored, which implies lesser chance for two Sn atoms to break the ether bonds probably because of interatomic repulsion between the Sn atoms which lessens the chance for them to interact with the surface oxygen atoms which is not the case for a lone Sn atom. An FML of Sn on ether resulted in Sn atoms unbonded and going away from the surface, hence no adsorption because of the same reasons.

It seems from the tables above that the most preferential configuration for Sn atoms on diamond (100) is QML (0.25

https://doi.org/10.1021/acs.jpcc.1c05973
J. Phys. Chem. C 2021, 125, 25165−25174

Table 4. Values of Electron Affinity, χ, and Adsorption Energy, E_{ads}, Calculated for Various Positions and at Different Surface Coverages of Sn on the OTD (100) Surface in the Ether Configuration

ether oxygen terminated	coverage (ML)	Sn configuration	adsorption energy, E_a (eV) per adsorbate	electron affinity, χ (eV)
	0.25	in between four O atoms	−5.9	−0.86
	0.5	ether	−5.6	2.31
	0.5	ketone	−5.27	−1.37
	1	ether	−4.6	1.88

Table 5. Values of Electron Affinity, χ, and Adsorption Energy, E_{ads}, Calculated for Various Positions and at Different Surface Coverages of Sn on the OTD (100) Surface in the Ketone Configuration

ketone oxygen terminated	coverage	Sn configuration	adsorption energy, E_a (eV) per adsorbate	electron affinity, χ (eV)
	0.25	in between four O atoms	−6.45	0.40
	0.5	ether	−5.8	−2
	0.5	ketone	−6.03	−1.37
	1	ether	−4.5	0.28

ML) of Sn atoms on top of the ketone-terminated oxygen atoms (can be seen in Figure 5b) which makes sense as it is expected that breaking a ketone bond would be easier for an Sn atom to bond with surface O than a more stable ether bond. However, this leads to a PEA value of 0.40 eV. It is the trend in the NEA that is important here not the absolute value as GGA is known to produce wrong estimates of electron affinity. Because the value of 0.40 is very small (very close to the negative scale), and it has been experimentally seen that the sub-ML Sn adsorption leads to NEA on the surface of diamond (100)[18] along with the fact that all other adsorption configurations (in the above Tables 4 and 5) result in NEA, hence it could be said that Sn leads to NEA on the surface of diamond (100) in most of the stable configurations. It can be concluded that Sn prefers ketone-terminated oxygen on the surface of diamond than the ether-terminated one as can be seen from the larger adsorption energy values in the tables. HML coverage of Sn is the coverage of interest as nearly all the experiments investigating the surface properties of Sn-terminated diamond would yield genuine insights into this field of study when the metal/metal oxide layer is under one ML, especially when the advanced spectroscopic techniques are used. HML coverage of Sn on the ketone-terminated diamond (can be seen in Figure 5c) also results in a large adsorption energy value of 6.03 eV with a large NEA value of −1.37 eV, which is an important and a hopeful outcome that sets a base for the future theoretical and experimental investigation into this topic.

The NEA values (more exactly trends) for Sn on bare and OTD (100) surfaces are comparable to the ones obtained for the hydrogen-terminated diamond and Li/LiO-terminated diamond (100) with larger adsorption energies implying stronger bonding between the surface species. An FML of Sn on ketone OTD resulted in Sn atoms unbonded and going away from the surface, hence no adsorption, similar to the ether OTD case.

To gain a further insight into the nature of the dipole at the surface, EP was generated for the most stable ketone-terminated diamond surface as shown in Figure 6.

Figure 6 shows the EP along the normal to the surface of diamond (100). There is a complex interaction at the surface as compared to the bare surface. The downswing (trough) depicts the positive side of the surface dipole which is centered on the Sn atom as expected and seen in the Mulliken charge analysis too (discussed below). Since O atoms are more electronegative than both C and Sn, they attract the charge density toward itself resulting in the centering of the negative side of the surface dipole between the C−O and O−Sn bonds in the form of δ_1^- and δ_2^+ (where it seems that $\delta_1^- > \delta_2^+$), respectively. This results in the net negative charge accumulation near the surface carbon atoms, giving rise to NEA on the surface of diamond.

The Mulliken bond population value of 0.04 indicates the ionic nature of the bond between surface-bonded O atoms and Sn atoms in the case of ether-terminated diamond with QML coverage along with an increase in the covalency (from 0.45 up to 0.74) of the bond between surface C and O atoms because of Sn adsorption. Mulliken charge analysis on the most stable configurations of Sn on OTD reveals the formation of a CO^-−Sn^+ dipole with Sn attaining a positive charge of 1.22e, O attaining a negative charge of −0.47e, and C attaining a positive charge of 0.45e. The bond length is further reduced between C and O atoms because of Sn adsorption which again indicates the increase in the covalency of the bond between the surface C and O and hence stronger bonding, in the case of ether-terminated diamond. However, in the case of ketone-terminated diamond the covalency between C and O atoms reduces considerably because of Sn adsorption. The bond length between C and O atoms increases which shows more tendency toward a single bonded character which is expected as Sn atoms would break the double bond (π bond) between C and O atoms. A similar trend can be seen in the case of the most stable HML coverage on the ketone-terminated diamond surface.

Projected Density of States (PDOS) Calculation. PDOS calculations are performed using the OptaDOS code[47] in CASTEP to show the density of electronic states for individual atoms in the optimized structure. The adsorption of Sn on the bare and oxygenated diamond (100) results in a significant decrease in the WF, as has been seen experimentally also, and NEA which occurs because of a shift in the electron density between the surface atoms.[18] In the case of Sn adsorption on the bare diamond surface, a simple explanation of a surface dipole, as mentioned in the earlier sections, can explain the mechanism of this shift, however, as has been seen in the case of OTD, any explanation to this phenomenon demands a further support. Here, PDOS calculations before and after the Sn adsorption on the OTD will help us to understand further the distribution of electron density at the surface which accounts for the shift in the WF of the diamond surface.

Figure 7a shows the PDOS structure for the bulk and surface carbon atoms in the bare diamond (100), taken from the center of the diamond slab and from the dimer row, respectively. Because of the sp3 bonds being distributed across the diamond lattice, there are indistinct, broader, and less intense peaks features present across the spectra especially toward the higher energy region. There are states within the band gap region of the diamond which originate from π and π^*

https://doi.org/10.1021/acs.jpcc.1c05973
J. Phys. Chem. C 2021, 125, 25165−25174

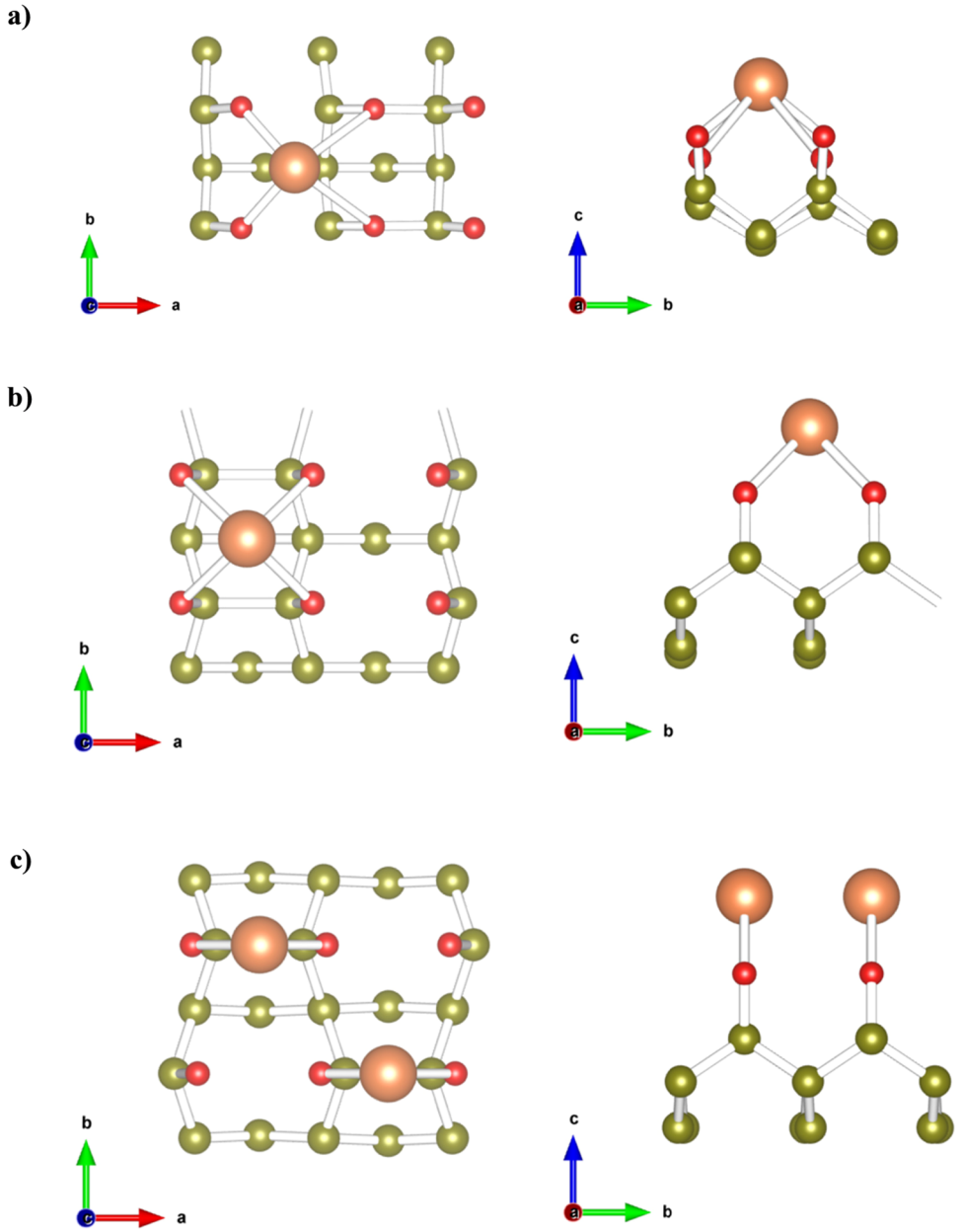

Figure 5. Geometry-optimized most stable output structures showing (a) QML (1 atom) Sn on the oxygen (ether) terminated diamond; no surface reconstruction has occurred because of Sn adsorption. (b) QML adsorption where one Sn is shared by four O (ketone) atoms (4 coordination) hence resulted in reconstruction (or C−C bond) on the surface. (c) HML adsorption, where each Sn atom is shared by two O (ketone) atoms (2 coordination), hence resulted in reconstruction (or C−C bond) on the surface. Green balls represent carbon atoms while red balls and orange balls represent oxygen and tin atoms, respectively. Adopted with modification from ref 18.

bonds of the surface carbon dimer rows. Figure 7b shows the PDOS spectra for the most stable QML of Sn adsorbed on the bare diamond (100) surface. The existence of a large peak which can be deconvoluted into a multiple-peak structure can be seen within the 20 to 25 eV region, indicating the tin-oxide structure on the surface of diamond. This feature can be a distinguishing factor between tin monoxide and tin dioxide as has been mentioned in the Methods section. This feature is analogous to that of Sn 4d peak structure seen in X-ray photoelectron spectroscopy spectra or the valence band structure of SnO on diamond.[18] There are states still present within the band gap of diamond, and a match between the surface C states and Sn states indicates that a covalent bonding between the two surface species is clearly visible. Figure 7c shows the typical PDOS structure for ketone-terminated diamond, which shows the density of states for bulk carbon, surface carbon, and oxygen atoms in the ketone configuration. Again, because of the sp^3 bonds being distributed across the diamond lattice, there are indistinct, broader, and less intense peak features between 5 and 15 eV corresponding to the sp^3 bonds than more localized features between −8 and 0 eV corresponding to sp^2 bonds. At higher energies, the PDOS presents similar distinct and sharp peaks for both surface C and O atoms at −6 and 24 eV, indicating the strong covalent bonding (sp^2 bonding character) between these species. In addition to these states, the surface oxygens have three sharp nonbonding peaks within the band gap at around −0.5, −2,

https://doi.org/10.1021/acs.jpcc.1c05973
J. Phys. Chem. C 2021, 125, 25165−25174

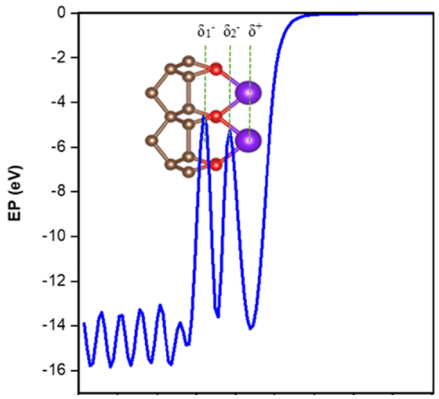

Figure 6. EP for the most stable configuration, that is, HML of Sn (ketone or on top) on oxygen (ketone)-terminated diamond (100). The large surface dipole apparent in the potential is projected onto the structure. It shows that the dipole is bond-centric as has been found in the case of LiO-terminated diamond[5] rather than atom-centric unlike H-terminated diamond. Here in this figure, brown balls represent carbon atoms while red balls and purple balls represent oxygen and tin atoms, respectively.

and −3.5 eV corresponding to the lone-pair electrons on the oxygens.

The adsorption of a HML of Sn on the ketone-terminated diamond surface results in a significant change in the density of states of the surface species, as can be seen in Figure 7d. The three sharp lone-pair oxygen levels have been substantially downshifted in energy and seem to overlap with the bulk levels, indicating charge transfer from Sn to the other surface species (−O−C) as discussed in EP analysis too. There is obvious evidence of match in PDOS spectra between surface C and O at many energy points which indicates strong covalent bonding between the species before Sn adsorption which seems to go away with Sn adsorption considerably indicating the breakage of the strong double bond between the surface C and O and formation of an O−Sn single bond as can be seen in an excellent match between all three surface species between − 20 and − 26 eV. This also shows the charge redistribution between the surface species that leads to the lowering of WF and NEA.

CONCLUSIONS

This work describes the surface and electronic structure of diamond (100) when Sn is adsorbed on bare and oxygen-terminated diamond in various coverages and configurations, which could serve as a foundation for any future theoretical and experimental investigation into Sn surface-doped diamond or Sn surface-terminated diamond for any application that demands lower WF thin films or diamond-based samples with NEA. DFT calculations were performed to determine the most stable position and coverage of Sn on bare and oxygen-terminated diamond (100). It was seen that most of the sites (whether on bare or OT diamond) exhibited NEA with large adsorption energies. There is a predominant covalent nature between Sn and surface C/surface O atoms, hence stronger bonding. A QML of Sn on bare diamond resulted in NEA with

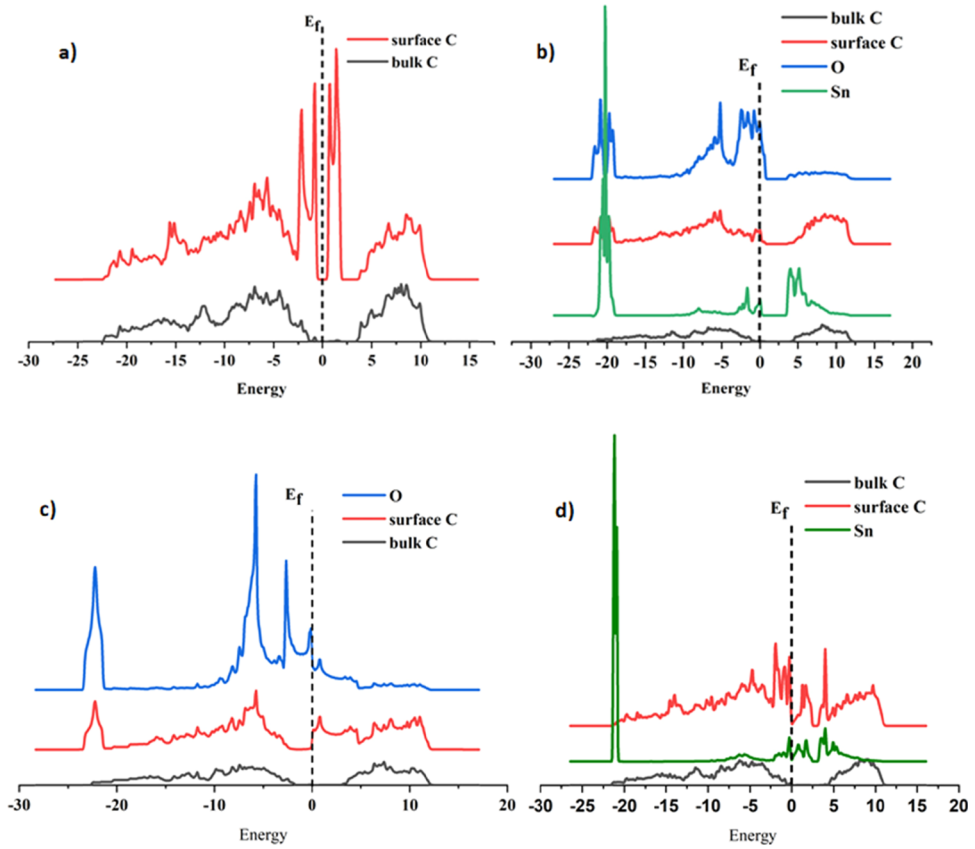

Figure 7. (a) PDOS for bulk C and surface C prior to Sn adsorption. (b) PDOS for the same layers after QML of Sn adsorption (shifted vertically for clarity). (c) PDOS for bulk C, surface C, and surface O (ketone) prior to Sn adsorption. (d) PDOS for the same layers after QML of Sn adsorption (shifted vertically for clarity). All energies are relative to the Fermi level at 0 eV.

https://doi.org/10.1021/acs.jpcc.1c05973
J. Phys. Chem. C 2021, 125, 25165−25174

a large adsorption energy while a HML of Sn on OTD has resulted in much larger NEA and adsorption energy, which is expected because oxygen inclusion increases the sticking coefficient and hence bond strength between the atoms. It was determined from the EP and the PDOS calculations that due to a shift in the electron density toward the more electronegative species or in other words due to the phenomenon of charge redistribution because of Sn adsorption, there is an accumulation of negative charge on or near the surface carbon atoms which results in NEA and a lower WF at the surface of diamond (100).

AUTHOR INFORMATION

Corresponding Author

Sami Ullah − *School of Physics, HH Wills Physics Laboratory and Bristol Centre for Functional Nanomaterials, University of Bristol, Bristol BS8 1TL, U.K.;* orcid.org/0000-0003-1999-0481; Email: Sami.ullah@bristol.ac.uk, owaisiameeni@gmail.com

Author

Neil Fox − *School of Physics, HH Wills Physics Laboratory, University of Bristol, Bristol BS8 1TL, U.K.; School of Chemistry, University of Bristol, Bristol BS8 1TS, U.K.*

Complete contact information is available at: https://pubs.acs.org/10.1021/acs.jpcc.1c05973

Author Contributions

The manuscript was written through contributions of all authors. All authors have given approval to the final version of the manuscript.

Notes

The authors declare no competing financial interest.

The data sets generated and/or analyzed during the current study are available from the corresponding author on reasonable request.

ACKNOWLEDGMENTS

This work was carried out using the computational facilities of the Advanced Computing Research Centre, University of Bristol—http://bris.ac.uk/acrc/. The structures were created and visualized using VESTA Software [57] and JMOL—http://jmol.org/. The authors acknowledge the Bristol NanoESCA Facility (EPSRC Strategic Equipment Grant EP/K035746/1 and EP/M000605/1) and staff, especially Dr. Jude Laverock and Dr. Gary wan for their useful insight regarding the topic. S.U. acknowledges the Ph.D. studentship funded through BCFN: The Zutshi Smith Scholarship, University of Bristol.

REFERENCES

(1) James, M. C.; Fogarty, F.; Zulkharnay, R.; Fox, N. A.; May, P. W. A Review of Surface Functionalisation of Diamond for Thermionic Emission Applications. *Carbon* **2021**, 532.

(2) Ashfold, M. N. R.; Goss, J. P.; Green, B. L.; May, P. W.; Newton, M. E.; Peaker, C. V. Nitrogen in Diamond. *Chem. Rev.* **2020**, *120*, 5745−5794.

(3) O'Donnell, K. M.; Martin, T. L.; Edmonds, M. T.; Tadich, A.; Thomsen, L.; Ristein, J.; Pakes, C. I.; Fox, N. A.; Ley, L. Photoelectron emission from lithiated diamond. *Phys. Status Solidi Appl. Mater. Sci.* **2014**, *211*, 2209−2222.

(4) Wan, G.; Cattelan, M.; Fox, N. A. Electronic structure tunability of diamonds by surface functionalization. *J. Phys. Chem. C* **2019**, 4168.

(5) O'Donnell, K. M.; Edmonds, M. T.; Ristein, J.; Tadich, A.; Thomsen, L.; Wu, Q. H.; Pakes, C. I.; Ley, L. Diamond Surfaces with Air-Stable Negative Electron Affinity and Giant Electron Yield Enhancement. *Adv. Funct. Mater.* **2013**, *23*, 5608−5614.

(6) O'Donnell, K. M.; Martin, T. L.; Allan, N. L. Light Metals on Oxygen-Terminated Diamond (100): Structure and Electronic Properties. *Chem. Mater.* **2015**, *27*, 1306−1315.

(7) Cui, J. B.; Ristein, J.; Stammler, M.; Janischowsky, K.; Kleber, G.; Ley, L. Hydrogen termination and electron emission from CVD diamond surfaces: A combined secondary electron emission, photoelectron emission microscopy, photoelectron yield, and field emission study. *Diamond Relat. Mater.* **2000**, *9*, 1143−1147.

(8) Takeuchi, D.; Ri, S.-G.; Kato, H.; Nebel, C. E.; Yamasaki, S. Negative electron affinity on hydrogen terminated diamond. *Phys. status solidi* **2005**, *202*, 2098−2103.

(9) Kawarada, H. Hydrogen-terminated diamond surfaces and interfaces. *Surf. Sci. Rep.* **1996**, *26*, 205−206.

(10) Baumann, P. K.; Nemanich, R. J. Electron affinity and Schottky barrier height of metal-diamond (100), (111), and (110) interfaces. *J. Appl. Phys.* **1998**, *83*, 2072−2082.

(11) Rezek, B.; Sauerer, C.; Nebel, C. E.; Stutzmann, M. Fermi level on hydrogen terminated diamond surfaces. *Appl. Phys. Lett.* **2003**, *82*, 2266−2268.

(12) Petrini, D.; Larsson, K. A theoretical study of the energetic stability and geometry of hydrogen- and oxygen-terminated diamond (100) surfaces. *J. Phys. Chem. C* **2007**, *111*, 795−801.

(13) Sque, S. J.; Jones, R.; Briddon, P. R. Structure, electronics, and interaction of hydrogen and oxygen on diamond surfaces. *Phys. Rev. B - Condens. Matter Mater. Phys.* **2006**, *73*, No. 085313.

(14) Baumann, P. K.; Nemanich, R. J. Surface cleaning, electronic states and electron affinity of diamond (100), (111) and (110) surfaces. *Surf. Sci.* **1998**, *409*, 320−335.

(15) Rutter, M.; Robertson, J. Ab initio calculation of electron affinities of diamond surfaces. *Phys. Rev. B - Condens. Matter Mater. Phys.* **1998**, *57*, 9241−9245.

(16) Kaviani, M.; Deák, P.; Aradi, B.; Frauenheim, T.; Chou, J. P.; Gali, A. Proper surface termination for luminescent near-surface NV centers in diamond. *Nano Lett.* **2014**, *14*, 4772−4777.

(17) O'Donnell, K. M.; Martin, T. L.; Fox, N. A.; Cherns, D. Ab initio investigation of lithium on the diamond C(100) surface. *Phys. Rev. B - Condens. Matter Mater. Phys.* **2010**, *82*, No. 115303.

(18) Ullah, S.; Wan, G.; Kouzios, C.; Woodgate, C.; Cattelan, M.; Fox, N. Structure and electronic properties of tin monoxide (SnO) and lithiated SnO terminated diamond (100) and its comparison with lithium oxide terminated diamond. *Appl. Surf. Sci.* **2021**, *559*, No. 149962.

(19) Shen, W.; Pan, Y.; Shen, S.; Li, H.; Zhang, Y.; Zhang, G. Electron affinity of boron-terminated diamond (001) surfaces: a density functional theory study. *J. Mater. Chem. C* **2019**, *7*, 9756.

(20) Sun, Z.; Yang, M.; Wang, X.; Wang, P.; Zhang, C.; Gao, N.; Li, H. Boron-terminated diamond (100) surfaces with promising structural and electronic properties. *Phys. Chem. Chem. Phys.* **2020**, *22*, 8060−8066.

(21) Maier, F.; Ristein, J.; Ley, L. Electron affinity of plasma-hydrogenated and chemically oxidized diamond (100) surfaces. *Phys. Rev. B - Condens. Matter Mater. Phys.* **2001**, *64*, No. 165411.

(22) Speranza, G.; Torrengo, S.; Miotello, A.; Minati, L.; Bernagozzi, I.; Ferrari, M.; Dipalo, M.; Kohn, E. XPS and UPS in situ study of oxygen thermal desorption from nanocrystalline diamond surface oxidized by different process. *Diamond Relat. Mater.* **2011**, *20*, 560−563.

(23) Stacey, A.; O'Donnell, K. M.; Chou, J. P.; Schenk, A.; Tadich, A.; Dontschuk, N.; Cervenka, J.; Pakes, C.; Gali, A.; Hoffman, A.; Prawer, S. Nitrogen Terminated Diamond. *Adv. Mater. Interfaces* **2015**, *2*, No. 1500079.

(24) Diederich, L.; Küttel, O. M.; Aebi, P.; Schlapbach, L. Electron affinity and work function of differently oriented and doped diamond surfaces determined by photoelectron spectroscopy. *Surf. Sci.* **1998**, *418*, 219−239.

(25) Yamaguchi, H.; Masuzawa, T.; Nozue, S.; Kudo, Y.; Saito, I.; Koe, I.; Kudo, M.; Yamada, T.; Takakuwa, Y.; Okano, K. Electron emission from conduction band of diamond with negative electron affinity. *Phys. Rev. B - Condens. Matter Mater. Phys.* **2009**, *80*, No. 165321.
(26) Diederich, L.; Aebi, P.; Küttel, O. M.; Schlapbach, L. NEA peak of the differently terminated and oriented diamond surfaces. *Surf. Sci.* **1999**, *424*, L314−L320.
(27) Takeuchia, D.; Kato, H.; Ri, G. S.; Yamada, T.; Vinod, P. R.; Hwang, D.; Nebel, C. E.; Okushi, H.; Yamasaki, S. Direct observation of negative electron affinity in hydrogen-terminated diamond surfaces. *Appl. Phys. Lett.* **2005**, *86*, 1−3.
(28) Baumann, P. K.; Nemanich, R. J. Electron emission from metal-diamond (100), (111) and (110) interfaces. *Diamond Relat. Mater.* **1998**, *7*, 612−619.
(29) Nie, J. L.; Xiao, H. Y.; Zu, X. T.; Gao, F. First principles calculations on Na and K-adsorbed diamond(1 0 0) surface. *Chem. Phys.* **2006**, *326*, 308−314.
(30) James, M. C.; Croot, A.; May, P. W.; Allan, N. L. Negative electron affinity from aluminium on the diamond (1 0 0) surface: A theoretical study. *J. Phys. Condens. Matter* **2018**, *30*, 235002.
(31) Köck, F. A. M.; Garguilo, J. M.; Nemanich, R. J. Imaging electron emission from diamond film surfaces: N-doped diamond vs. nanostructured diamond. *Diamond Relat. Mater.* **2001**, *10*, 1714−1718.
(32) Baumann, P. K.; Nemanich, R. J. Characterization of copper-diamond (100), (111), and (110) interfaces: Electron affinity and Schottky barrier. *Phys. Rev. B* **1998**, *58*, 1643−1654.
(33) Baumann, P. K.; Nemanich, R. J. Characterization of cobalt-diamond (100) interfaces: electron affinity and Schottky barrier. *Appl. Surf. Sci.* **1996**, *104-105*, 267−273.
(34) Koeck, F. A. M.; Nemanich, R. J.; Lazea, A.; Haenen, K. Thermionic electron emission from low work-function phosphorus doped diamond films. *Diamond Relat. Mater.* **2009**, *18*, 789−791.
(35) Ullah, S.; Cullingford, L.; Zhang, T.; Wong, J. R.; Wan, G.; Cattelan, M.; Fox, N. An investigation into the surface termination and near-surface bulk doping of oxygen-terminated diamond with lithium at various annealing temperatures. *MRS Advances* **2021**, 311−320.
(36) James, M. C.; May, P. W.; Allan, N. L. *Ab initio* study of negative electron affinity from light metals on the oxygen-terminated diamond (1 1 1) surface. *J. Phys. Condens. Matter* **2019**, *31*, 295002.
(37) Schenk, A.; Tadich, A.; Sear, M.; O'Donnell, K. M.; Ley, L.; Stacey, A.; Pakes, C. Formation of a silicon terminated (100) diamond surface. *Appl. Phys. Lett.* **2015**, *106*, 191603.
(38) Schenk, A. K.; Tadich, A.; Sear, M. J.; Qi, D.; Wee, A. T. S.; Stacey, A.; Pakes, C. I. The surface electronic structure of silicon terminated (100) diamond. *Nanotechnology* **2016**, *27*, No. 275201.
(39) Sear, M. J.; Schenk, A. K.; Tadich, A.; Spencer, B. J.; Wright, C. A.; Stacey, A.; Pakes, C. I. Germanium terminated (1 0 0) diamond. *J. Phys. Condens. Matter* **2017**, *29*, 145002.
(40) O'Donnell, K. M.; Martin, T. L.; Allan, N. L. Light metals on oxygen-terminated diamond (100): Structure and electronic properties. *Chem. Mater.* **2015**, *27*, 1306−1315.
(41) Tiwari, A. K.; Goss, J. P.; Briddon, P. R.; Wright, N. G.; Horsfall, A. B.; Rayson, M. J. Effect of different surface coverages of transition metals on the electronic and structural properties of diamond. *Phys. Status Solidi Appl. Mater. Sci.* **2012**, *209*, 1697−1702.
(42) Fogarty, F. *Renewable Energy − Low Temperature Thermionic Emission from Modified Diamond Surfaces*. (2020).
(43) Clark, S. J.; Segall, M. D.; Pickard, C. J.; Hasnip, P. J.; Probert, M. I. J.; Refson, K.; Payne, M. C. First principles methods using CASTEP. *Zeitschrift fur Krist* **2005**, *220*, 567−570.
(44) Perdew, J. P.; Burke, K.; Ernzerhof, M. Generalized gradient approximation made simple. *Phys. Rev. Lett.* **1996**, *77*, 3865−3868.
(45) Vanderbilt, D. Soft self-consistent pseudopotentials in a generalized eigenvalue formalism. *Phys. Rev. B* **1990**, *41*, 7892−7895.
(46) Monkhorst, H. J.; Pack, J. D. Special points for Brillouin-zone integrations. *Phys. Rev. B* **1976**, *13*, 5188−5192.
(47) Morris, A. J.; Nicholls, R. J.; Pickard, C. J.; Yates, J. R. OptaDOS: A tool for obtaining density of states, core-level and optical spectra from electronic structure codes. *Comput. Phys. Commun.* **2014**, *185*, 1477−1485.
(48) Fall, C. J.; Binggeli, N.; Baldereschi, A. Deriving accurate work functions from thin-slab calculations. *J. Phys. Condens. Matter* **1999**, *11*, 2689−2696.
(49) James, M. C. *Aluminium and Oxygen Termination of Diamond for Thermionic Applications*. (2019).
(50) Martin, T. L. *Lithium oxygen termination as a negative electron affinity surface on diamond : a computational and photoemission study*. (2011).
(51) Qi, D.; Liu, L.; Gao, X.; Ouyang, T.; Chen, S.; Loh, K. P.; Wee, A. T. S. Tuning the electron affinity and secondary electron emission of diamond (100) surfaces by diels-alder reaction. *Langmuir* **2007**, *23*, 9722−9727.
(52) Furthmüller, J.; Hafner, J.; Kresse, G. Dimer reconstruction and electronic surface states on clean and hydrogenated diamond (100) surfaces. *Phys. Rev. B - Condens. Matter Mater. Phys.* **1996**, *53*, 7334−7351.
(53) Van Der Weide, J.; Zhang, Z.; Baumann, P. K.; Wensell, M. G.; Bernholc, J.; Nemanich, R. J. Negative-electron-affinity effects on the diamond (100) surface. *Phys. Rev. B* **1994**, *50*, 5803−5806.
(54) Zheng, X. M.; Smith, P. V. The stable configurations for oxygen chemisorption on the diamond (100) and (111) surfaces. *Surf. Sci.* **1992**, *262*, 219−234.
(55) Levine, J. D. Structural and electronic model of negative electron affinity on the Si/Cs/O surface. *Surf. Sci.* **1973**, *34*, 90−107.

https://doi.org/10.1021/acs.jpcc.1c05973
J. Phys. Chem. C 2021, 125, 25165−25174